HHS Public Access

Author manuscript

Inorg Chem. Author manuscript; available in PMC 2022 August 12.

Published in final edited form as:

Inorg Chem. 2022 January 17; 61(2): 801–806. doi:10.1021/acs.inorgchem.1c03670.

Chelating the Alpha Therapy Radionuclides $^{225}Ac^{3+}$ and $^{213}Bi^{3+}$ with 18-Membered Macrocyclic Ligands Macrodipa and Py-Macrodipa

Aohan Hu[†], **Victoria Brown**[‡], **Samantha N. MacMillan**[†], **Valery Radchenko**[§,⊥], **Hua Yang**[§], **Luke Wharton**[⊥,§], **Caterina F. Ramogida**[‡,§], **Justin J. Wilson**[†]

[†]Department of Chemistry and Chemical Biology, Cornell University, Ithaca, New York 14853, United States

[‡]Department of Chemistry, Simon Fraser University, Burnaby, British Columbia V5A 1S6, Canada

[§]Life Sciences Division, TRIUMF, Vancouver, British Columbia V6T 2A3, Canada

[⊥]Department of Chemistry, University of British Columbia, Vancouver, British Columbia V6T 1Z1, Canada

Abstract

The radionuclides $^{225}Ac^{3+}$ and $^{213}Bi^{3+}$ possess favorable physical properties for targeted alpha therapy (TAT), a therapeutic approach that leverages α radiation to treat cancers. A chelator that effectively binds and retains these radionuclides is required for this application. The development of ligands that can be used for this purpose, however, is challenging because the large ionic radii and charge-diffuse nature of these metal ions give rise to weaker metal-ligand interactions. In this study, we evaluated two 18-membered macrocyclic chelators, macrodipa and py-macrodipa, for their ability to complex $^{225}Ac^{3+}$ and $^{213}Bi^{3+}$. Their coordination chemistry with Ac^{3+} was probed computationally and with Bi^{3+} experimentally via NMR spectroscopy and X-ray crystallography. Furthermore, radiolabeling studies were conducted, revealing the efficient incorporation of both $^{225}Ac^{3+}$ and $^{213}Bi^{3+}$ by py-macrodipa that matches or surpasses the well-known chelators macropa and DOTA. Incubation in human serum at 37 °C showed that ~90% of the $^{225}Ac^{3+}$–py-macrodipa complex dissociates after 1 d. The Bi^{3+}–py-macrodipa complex possesses remarkable kinetic inertness in an EDTA transchelation challenge study, surpassing that of Bi^{3+}–macropa. This work establishes py-macrodipa as a valuable candidate for $^{213}Bi^{3+}$ TAT, providing further motivation for its implementation within new radiopharmaceutical agents.

Corresponding Author Justin J. Wilson – Department of Chemistry and Chemical Biology, Cornell University, Ithaca, New York 14853, United States; jjw275@cornell.edu.

The authors declare no competing financial interest.

Supporting Information

The Supporting Information is available free of charge at https://pubs.acs.org/doi/xxxxxxx.

Experimental procedures and supplementary data (PDF)

Crystallographic data for Bi^{3+}–macrodipa and Bi^{3+}–py-macrodipa (CIF)

Geometry outputs for DFT-optimized structures (ZIP)

Accession Codes

CCDC 2124116–2124117 contain the supplementary crystallographic data for this paper. These data can be obtained free of charge via www.ccdc.cam.ac.uk/data_request/cif, or by data_request@ccdc.cam.ac.uk, or by contacting The Cambridge Crystallographic Data Centre, 12 Union Road, Cambridge CB2 1EZ, UK; fax: + 44 1223 336033.

Graphical Abstract

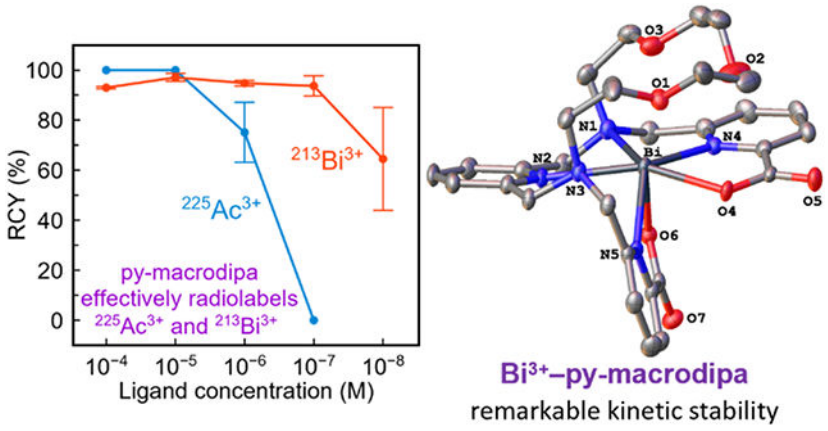

Targeted alpha therapy (TAT) is a promising therapeutic strategy that leverages α-particle-emitting radionuclides to annihilate tumor cells. Compared to conventional internal radiotherapy using β-particle emitters, the implementation of significantly more massive α particles, which deposit their energy over much shorter distances, provides key advantages. The short range of α radiation can yield enhanced selectivity for targeted cancer cells, while minimizing damage to surrounding healthy cells. Moreover, the very large linear energy transfer (LET) of α particles is significantly more effective in causing lethal DNA double strand breaks that kill cancer cells in a more efficacious manner compared to the lower-LET β particles.[1-6]

To date, over eight radionuclides have been identified as potential candidates for use in TAT based on their decay properties and production routes.[7] Among these nuclides, $^{225}Ac^{3+}$ and $^{213}Bi^{3+}$ have received considerable attention that has manifested in clinical studies.[8-10] ^{225}Ac ($t_{1/2}$ = 9.9 d) emits four α particles through its decay chain, a property that confers it with high cytotoxic potency. Its 9.9-day half-life is also well matched with the in vivo circulation timescales of macromolecular targeting vectors like antibodies.[11,12] ^{213}Bi ($t_{1/2}$ = 45.6 min), a daughter of $^{225}Ac^{3+}$, emits one α particle through its decay chain and can be conveniently obtained from $^{225}Ac/^{213}Bi$ generators.[13] Its shorter half-life can be optimally matched to small-molecule targeting vectors, rendering it useful for different systems than those used for $^{225}Ac^{3+}$.[14,15]

To convert these promising radionuclides into useful radiotherapeutic agents, a chelator that efficiently binds and stably retains them is required.[16,17] The development of chelators for large metal ions like Ac^{3+} and Bi^{3+}, however, is challenging, partly because their low charge density weakens electrostatic interactions with ligand donor atoms.

We recently reported a new ligand called macrodipa[18] and its second-generation analogue py-macrodipa[19] (Chart 1). These “macrodipa-type” chelators feature a unique “dual size selectivity”, characterized by their good affinities for both the large and small rare-earth metal ions (Ln^{3+}). This unusual selectivity profile arises from a significant conformational toggle that occurs when they form complexes with Ln^{3+} ions of different sizes. Large

Ln^{3+} form 10-coordinate, nearly C_2-symmetric complexes (Conformation A), whereas an 8-coordinate, asymmetric complex arises for small Ln^{3+} (Conformation B).[18,19] We have further demonstrated that this property makes py-macrodipa a valuable candidate for nuclear medicine applications with both $^{135}La^{3+}$ and $^{44}Sc^{3+}$, Ln^{3+} radiometal ions with the largest and smallest ionic radii within this series.[19]

Based on this successful application of macrodipa and py-macrodipa for the Ln^{3+} ions, we sought to evaluate these ligands with biomedically relevant ions beyond the Ln^{3+} series, namely Ac^{3+} and Bi^{3+}. The potentials of both chelators for TAT applications using their radioisotopes $^{225}Ac^{3+}$ and $^{213}Bi^{3+}$ were determined and benchmarked to those of the well-known chelators macropa and DOTA (Chart 1), which have established precedence for nuclear medicine applications with these radiometals.[20-23]

We assessed the coordination chemistry of these ligands with stable Bi^{3+}. The ^{1}H and $^{13}C\{^{1}H\}$ NMR spectra of their Bi^{3+} complexes (Bi^{3+}–macrodipa and Bi^{3+}–py-macrodipa) were acquired in D_2O (Figures 1 and S1-S4). These spectra reveal the presence of a single, well-resolved species that lacks symmetry for both complexes. Thus, Bi^{3+}–macrodipa and Bi^{3+}–py-macrodipa most likely attain the asymmetric Conformation B, which is the preferred binding mode of these ligands for small Ln^{3+} (Figure S5-S6).

As further validation, we characterized Bi^{3+}–macrodipa and Bi^{3+}–py-macrodipa by X-ray crystallography (Figure 2). The crystal structures of these complexes confirm that they attain the asymmetric Conformation B, consistent with our observations from NMR spectroscopy. Like their NMR spectra, these Bi^{3+} structures are comparable to those of the small Ln^{3+} analogues, Lu^{3+}–macrodipa and Sc^{3+}–py-macrodipa, with respect to the orientation of the picolinate donors and the lack of full engagement of all six macrocycle donor atoms.[18,19] A key difference between these Ln^{3+} and Bi^{3+} structures, however, is the absence of a coordinated water molecule in the latter. This void is most likely a consequence of the stereochemical activity[24,25] of the Bi^{3+} $6s^2$ lone pair. These observations that Bi^{3+}–macrodipa and Bi^{3+}–py-macrodipa attain the asymmetric Conformation B rather than the symmetric Conformation A is somewhat surprising based on the similar ionic radii of Bi^{3+} and La^{3+},[26,27] a representative large Ln^{3+}. This result suggests that the stereochemical activity of the $6s^2$ lone pair plays a pronounced role in mediating the preferred conformations of these Bi^{3+} complexes.

Experimental characterization of Ac^{3+} complexes is challenging due to the high radioactivity and extremely limited availability of its longest-lived isotope ^{227}Ac ($t_{1/2}$ = 21.8 y).[28] Thus instead, we probed the structures of Ac^{3+}–macrodipa and Ac^{3+}–py-macrodipa computationally using density functional theory (DFT) with *Gaussian 16*.[29] The hybrid TPSSh functional,[30] which has been validated for studying Ac^{3+} chemistry,[31,32] was adopted. A large-core relativistic effective core potential (LCRECP) and the associated basis set was assigned to the Ac^{3+} center,[33-35] whereas the 6-31G(d,p) basis set[36,37] was applied to all other lighter atoms. Aqueous solvation effects were accounted for with the SMD solvation model.[38]

Because the ionic radii and coordination chemistry of Ac^{3+} and La^{3+} are similar,[28] we optimized Ac^{3+}–macrodipa and Ac^{3+}–py-macrodipa starting from the geometries of the corresponding La^{3+} complexes, which attain the symmetric Conformation A.[18,19] Within these structures (Figure 3), the Ac–O interatomic distances are 2.45–2.48 Å for negatively charged O and 2.70–2.79 Å for neutral O, whereas the Ac–N interactions range from 2.76–2.92 Å. These calculated distances are in expectation with experimentally measured Ac–O and Ac–N interatomic distances.[39-43] Additionally, we optimized both complexes in Conformation B. Consistent with our expectations, Conformation B is energetically unfavored for both complexes (Table S2).

Having established the coordination chemistry of these ligands, we next carried out radiolabeling studies to evaluate their potential value for $^{225}Ac^{3+}$ and $^{213}Bi^{3+}$ TAT in comparison to the state-of-the-art chelators macropa and DOTA. These radionuclides were produced and purified according to previously-described protocols.[44-46]

Different concentrations of macrodipa, py-macrodipa, macropa, and DOTA were combined with pH 5.5–6 buffered solutions containing either 20–40 or 30–300 kBq of $^{225}Ac^{3+}$ and $^{213}Bi^{3+}$ at ambient or elevated temperature, and the radiochemical yields (RCYs) were determined by radio-TLC. The concentration-dependent RCYs for these four chelators are summarized in Figure 4. For both radionuclides, py-macrodipa is able to achieve significantly higher RCYs than its analogue macrodipa and the conventional chelator DOTA, which also required high temperatures for radiolabeling. RCYs of approximately 75% and 65% are obtained when using low py-macrodipa concentrations of 10^{-6} M and 10^{-8} M for $^{225}Ac^{3+}$ and $^{213}Bi^{3+}$, respectively. With respect to $^{225}Ac^{3+}$ chelation, py-macrodipa was slightly less effective than macropa, but was better at radiolabeling $^{213}Bi^{3+}$. We also performed $^{225}Ac^{3+}$ radiolabeling with macrodipa and py-macrodipa at pH 7 (Table S3). Under this condition, both chelators were able to access greater RCYs, but still failed to surpass macropa. Overall, these studies show that py-macrodipa effectively radiolabels both $^{225}Ac^{3+}$ and $^{213}Bi^{3+}$ under mild conditions.

We next assessed the kinetic inertness of $^{225}Ac^{3+}$–py-macrodipa by incubating it in human serum at 37 °C (Table S5). These studies show that $^{225}Ac^{3+}$–py-macrodipa is fairly labile, as ~90% of the complex dissociated after 1 d. By contrast, $^{225}Ac^{3+}$–macropa remained 98% intact in human serum after 5 d. This excellent kinetic inertness is consistent to a previously reported serum challenge on $^{225}Ac^{3+}$–macropa.[20] Hence, despite the efficient radiolabeling properties of py-macrodipa, it is not an optimal candidate for TAT applications with $^{225}Ac^{3+}$.

Because $^{213}Bi^{3+}$ decays quickly ($t_{1/2}$ = 45.6 min), probing the $^{213}Bi^{3+}$ complex kinetic inertness by this serum challenge assay is impractical. Instead, we performed a transchelation challenge assay[19-21,47-49] on the macrodipa, py-macrodipa, and macropa complexes with stable Bi^{3+}. The transchelation reactions of these Bi^{3+} complexes were monitored by UV–Vis spectroscopy in the presence of a 10-fold excess EDTA, a ligand with high affinity for Bi^{3+},[50,51] at pH 5.0 and 25 °C. Under this condition, the Bi^{3+} ion is transchelated by EDTA, following pseudo-first-order kinetics. The resulting half-lives ($t_{1/2}$) for this transchelation process, a comparative measure of complex kinetic inertness, are shown in Table 1. Bi^{3+}–macrodipa is kinetically labile to this transchelation challenge. The

kinetic inertness of Bi^{3+}–py-macrodipa is remarkably enhanced, as reflected by a $t_{1/2}$ of 13 d. Moreover, its inertness is greater than that of Bi^{3+}–macropa, indicating that py-macrodipa is a promising candidate for TAT applications with $^{213}Bi^{3+}$.

In summary, we evaluated the viability of macrodipa and py-macrodipa as chelators for $^{225}Ac^{3+}$ and $^{213}Bi^{3+}$. Their coordination chemistry with Ac^{3+} and Bi^{3+} were characterized computationally and experimentally, respectively. Our radiolabeling studies revealed that py-macrodipa is highly effective at radiolabeling both radiometals, outperfoming both macrodipa and DOTA. Although the lability of Ac^{3+}–py-macrodipa precludes its use with $^{225}Ac^{3+}$ in nuclear medicine, the efficient formation and high stability of Bi^{3+}–py-macrodipa, which surpasses Bi^{3+}–macropa, suggests that this ligand is a valuable candidate for $^{213}Bi^{3+}$ chelation. These results highlight that py-macrodipa joins other promising candidates for $^{213}Bi^{3+}$ chelation that have arisen in recent years.[21,52-60] Ongoing work is directed towards the synthesis of a bifunctional analogue of py-macrodipa to apply this chelator in TAT, as well as the development of “macrodipa-type” chelators with enhanced Ac^{3+} complex stabilities.

Supplementary Material

Refer to Web version on PubMed Central for supplementary material.

ACKNOWLEDGMENT

This research was supported by the National Institutes of Biomedical Imaging and Bioengineering of the National Institutes of Health under Award Numbers R21EB027282 and R01EB029259, as well as the Research Corporation for Science Advancement through a Cottrell Research Scholar Award to J.J.W. This research made use of the NMR Facility at Cornell University, which was supported, in part, by the U.S. National Science Foundation under award number CHE-1531632. TRIUMF receives funding via a contribution agreement with the Natural Research Council of Canada. The authors acknowledge the TRIUMF actinium-production team for their work to produce and isolate ^{225}Ac from the 500 MeV Isotope Production Facility. V.B. was funded by a Natural Sciences and Engineering Research Council (NSERC) Canada Graduate Scholarship – Masters (CGS-M).

REFERENCES

(1). Brechbiel MW Targeted α-Therapy: Past, Present, Future? Dalton Trans. 2007, 4918–4928. [PubMed: 17992276]

(2). Kim Y-S; Brechbiel MW An Overview of Targeted Alpha Therapy. Tumor Biol. 2012, 33, 573–590.

(3). Seidl C Radioimmunotherapy with α-Particle-Emitting Radionuclides. Immunotherapy 2014, 6, 431–458. [PubMed: 24815783]

(4). Guerra Liberal FDC; O’Sullivan JM; McMahon SJ; Prise KM Targeted Alpha Therapy: Current Clinical Applications. Cancer Biother. Radiopharm 2020, 35, 404–417. [PubMed: 32552031]

(5). Radchenko V; Morgenstern A; Jalilian AR; Ramogida CF; Cutler C; Duchemin C; Hoehr C; Haddad F; Bruchertseifer F; Gausemel H; Yang H; Osso JA; Washiyama K; Czerwinski K; Leufgen K; Pruszyński M; Valzdorf O; Causey P; Schaffer P; Perron R; Maxim S; Wilbur DS; Stora T; Li Y Production and Supply of α-Particle–Emitting Radionuclides for Targeted α-Therapy. J. Nucl. Med 2021, 62, 1495–1503. [PubMed: 34301779]

(6). Yang H; Wilson JJ; Orvig C; Li Y; Wilbur DS; Ramogida C; Radchenko V; Schaffer P Harnessing Alpha-Emitting Radionuclides for Therapy: Radiolabeling Method Review. J. Nucl. Med 2021, doi: jnumed.121.262687.

(7). Eychenne R; Chérel M; Haddad F; Guérard F; Gestin J-F Overview of the Most Promising Radionuclides for Targeted Alpha Therapy: The “Hopeful Eight”. Pharmaceutics 2021, 13, 906. [PubMed: 34207408]

(8). Morgenstern A; Apostolidis C; Kratochwil C; Sathekge M; Krolicki L; Bruchertseifer F An Overview of Targeted Alpha Therapy with ^{225}Actinium and ^{213}Bismuth. Curr. Radiopharm 2018, 11, 200–208. [PubMed: 29732998]

(9). Bruchertseifer F; Kellerbauer A; Malmbeck R; Morgenstern A Targeted Alpha Therapy with Bismuth-213 and Actinium-225: Meeting Future Demand. J. Labelled Compd. Radiopharm 2019, 62, 794–802.

(10). Morgenstern A; Apostolidis C; Bruchertseifer F Supply and Clinical Application of Actinium-225 and Bismuth-213. Semin. Nucl. Med 2020, 50, 119–123. [PubMed: 32172796]

(11). Geerlings MW; Kaspersen FM; Apostolidis C; van der Hout R The Feasibility of ^{225}Ac as a Source of α-Particles in Radioimmunotherapy. Nucl. Med. Commun 1993, 14, 121–125. [PubMed: 8429990]

(12). Thiele NA; Wilson JJ Actinium-225 for Targeted α Therapy: Coordination Chemistry and Current Chelation Approaches. Cancer Biother. Radiopharm 2018, 33, 336–348. [PubMed: 29889562]

(13). Morgenstern A; Bruchertseifer F; Apostolidis C Bismuth-213 and Actinium-225 – Generator Performance and Evolving Therapeutic Applications of Two Generator-Derived Alpha-Emitting Radioisotopes. Curr. Radiopharm 2012, 5, 221–227. [PubMed: 22642390]

(14). Hassfjell S; Brechbiel MW The Development of the α-Particle Emitting Radionuclides ^{212}Bi and ^{213}Bi, and Their Decay Chain Related Radionuclides, for Therapeutic Applications. Chem. Rev 2001, 101, 2019–2036. [PubMed: 11710239]

(15). Ahenkorah S; Cassells I; Deroose CM; Cardinaels T; Burgoyne AR; Bormans G; Ooms M; Cleeren F Bismuth-213 for Targeted Radionuclide Therapy: From Atom to Bedside. Pharmaceutics 2021, 13, 599. [PubMed: 33919391]

(16). Price EW; Orvig C Matching Chelators to Radiometals for Radiopharmaceuticals. Chem. Soc. Rev 2014, 43, 260–290. [PubMed: 24173525]

(17). Radiopharmaceutical Chemistry; Lewis JS, Windhorst AD, Zeglis BM, Eds.; Springer Nature Switzerland AG: Cham, Switzerland, 2019.

(18). Hu A; MacMillan SN; Wilson JJ Macrocyclic Ligands with an Unprecedented Size-Selectivity Pattern for the Lanthanide Ions. J. Am. Chem. Soc 2020, 142, 13500–13506. [PubMed: 32697907]

(19). Hu A; Aluicio-Sarduy E; Brown V; MacMillan SN; Becker KV; Barnhart TE; Radchenko V; Ramogida CF; Engle JW; Wilson JJ Py-Macrodipa: A Janus Chelator Capable of Binding Medicinally Relevant Rare-Earth Radiometals of Disparate Sizes. J. Am. Chem. Soc 2021, 143, 10429–10440. [PubMed: 34190542]

(20). Thiele NA; Brown V; Kelly JM; Amor-Coarasa A; Jermilova U; MacMillan SN; Nikolopoulou A; Ponnala S; Ramogida CF; Robertson AKH; Rodríguez-Rodríguez C; Schaffer P; Williams C Jr.; Babich JW; Radchenko V; Wilson JJ An Eighteen-Membered Macrocyclic Ligand for Actinium-225 Targeted Alpha Therapy. Angew. Chem., Int. Ed 2017, 56, 14712–14717.

(21). Fiszbein DJ; Brown V; Thiele NA; Woods JJ; Wharton L; MacMillan SN; Radchenko V; Ramogida CF; Wilson JJ Tuning the Kinetic Inertness of Bi^{3+} Complexes: The Impact of Donor Atoms on Diaza-18-Crown-6 Ligands as Chelators for ^{213}Bi Targeted Alpha Therapy. Inorg. Chem 2021, 60, 9199–9211. [PubMed: 34102841]

(22). McDevitt MR; Ma D; Simon J; Frank RK; Scheinberg DA Design and Synthesis of ^{225}Ac Radioimmunopharmaceuticals. Appl. Radiat. Isot 2002, 57, 841–847. [PubMed: 12406626]

(23). Norenberg JP; Krenning BJ; Konings IRHM; Kusewitt DF; Nayak TK; Anderson TL; de Jong M; Garmestani K; Brechbiel MW; Kvols LK ^{213}Bi-[$DOTA^0$, Tyr^3]Octreotide Peptide Receptor Radionuclide Therapy of Pancreatic Tumors in a Preclinical Animal Model. Clin. Cancer Res 2006, 12, 897–903. [PubMed: 16467104]

(24). Shimoni-Livny L; Glusker JP; Bock CW Lone Pair Functionality in Divalent Lead Compounds. Inorg. Chem 1998, 37, 1853–1867.

(25). Pujales-Paradela R; Rodríguez-Rodríguez A; Gayoso-Padula A; Brandariz I; Valencia L; Esteban-Gómez D; Platas-Iglesias C On the Consequences of the Stereochemical Activity of the Bi(iii) $6s^2$ Lone Pair in Cyclen-Based Complexes. The [Bi(DO3A)] Case. Dalton Trans. 2018, 47, 13830–13842. [PubMed: 30230496]

(26). Shannon RD Revised Effective Ionic Radii and Systematic Studies of Interatomic Distances in Halides and Chalcogenides. Acta Crystallogr., Sect. A: Found. Adv 1976, 32, 751–767.

(27). Näslund J; Persson I; Sandström M Solvation of the Bismuth(III) Ion by Water, Dimethyl Sulfoxide, *N,N′*-Dimethylpropyleneurea, and *N,N*-Dimethylthioformamide. An EXAFS, Large-Angle X-ray Scattering, and Crystallographic Structural Study. Inorg. Chem 2000, 39, 4012–4021. [PubMed: 11198855]

(28). Deblonde GJ-P; Zavarin M; Kersting AB The Coordination Properties and Ionic Radius of Actinium: A 120-Year-Old Enigma. Coord. Chem. Rev 2021, 446, 214130.

(29). Frisch MJ; Trucks GW; Schlegel HB; Scuseria GE; Robb MA; Cheeseman JR; Scalmani G; Barone V; Petersson GA; Nakatsuji H; Li X; Caricato M; Marenich AV; Bloino J; Janesko BG; Gomperts R; Mennucci B; Hratchian HP; Ortiz JV; Izmaylov AF; Sonnenberg JL; Williams-Young D; Ding F; Lipparini F; Egidi F; Goings J; Peng B; Petrone A; Henderson T; Ranasinghe D; Zakrzewski VG; Gao J; Rega N; Zheng G; Liang W; Hada M; Ehara M; Toyota K; Fukuda R; Hasegawa J; Ishida M; Nakajima T; Honda Y; Kitao O; Nakai H; Vreven T; Throssell K; Montgomery JA Jr.; Peralta JE; Ogliaro F; Bearpark MJ; Heyd JJ; Brothers EN; Kudin KN; Staroverov VN; Keith TA; Kobayashi R; Normand J; Raghavachari K; Rendell AP; Burant JC; Iyengar SS; Tomasi J; Cossi M; Millam JM; Klene M; Adamo C; Cammi R; Ochterski JW; Martin RL; Morokuma K; Farkas O; Foresman JB; Fox DJ Gaussian 16, Revision C. 01; Gaussian, Inc.: Wallingford, CT, 2016.

(30). Tao J; Perdew JP; Staroverov VN; Scuseria GE Climbing the Density Functional Ladder: Nonempirical Meta–Generalized Gradient Approximation Designed for Molecules and Solids. Phys. Rev. Lett 2003, 91, 146401. [PubMed: 14611541]

(31). Kovács A Theoretical Study of Actinide Complexes with Macropa. ACS Omega 2020, 5, 26431–26440. [PubMed: 33110971]

(32). Kovács A Theoretical Study of Actinide(III)-DOTA Complexes. ACS Omega 2021, 6, 13321–13330. [PubMed: 34056480]

(33). Küchle W; Dolg M; Stoll H; Preuss H Energy-Adjusted Pseudopotentials for the Actinides. Parameter Sets and Test Calculations for Thorium and Thorium Monoxide. J. Chem. Phys 1994, 100, 7535–7542.

(34). Cao X; Dolg M; Stoll H Valence Basis Sets for Relativistic Energy-Consistent Small-Core Actinide Pseudopotentials. J. Chem. Phys 2003, 118, 487–496.

(35). Cao X; Dolg M Segmented Contraction Scheme for Small-Core Actinide Pseudopotential Basis Sets. J. Mol. Struct.: THEOCHEM 2004, 673, 203–209.

(36). Hehre WJ; Ditchfield R; Pople JA Self-Consistent Molecular Orbital Methods. XII. Further Extensions of Gaussian-Type Basis Sets for Use in Molecular Orbital Studies of Organic Molecules. J. Chem. Phys 1972, 56, 2257–2261.

(37). Hariharan PC; Pople JA The Influence of Polarization Functions on Molecular Orbital Hydrogenation Energies. Theor. Chim. Acta 1973, 28, 213–222.

(38). Marenich AV; Cramer CJ; Truhlar DG Universal Solvation Model Based on Solute Electron Density and on a Continuum Model of the Solvent Defined by the Bulk Dielectric Constant and Atomic Surface Tensions. J. Phys. Chem. B 2009, 113, 6378–6396. [PubMed: 19366259]

(39). Ferrier MG; Batista ER; Berg JM; Birnbaum ER; Cross JN; Engle JW; La Pierre HS; Kozimor SA; Lezama Pacheco JS; Stein BW; Stieber SCE; Wilson JJ Spectroscopic and Computational Investigation of Actinium Coordination Chemistry. Nat. Commun 2016, 7, 12312. [PubMed: 27531582]

(40). Ferrier MG; Stein BW; Batista ER; Berg JM; Birnbaum ER; Engle JW; John KD; Kozimor SA; Lezama Pacheco JS; Redman LN Synthesis and Characterization of the Actinium Aquo Ion. ACS Cent. Sci. 2017, 3, 176–185. [PubMed: 28386595]

(41). Ferrier MG; Stein BW; Bone SE; Cary SK; Ditter AS; Kozimor SA; Lezama Pacheco JS; Mocko V; Seidler GT The Coordination Chemistry of Cm^{III}, Am^{III}, and Ac^{III} in Nitrate Solutions: an Actinide L_3-Edge EXAFS Study. Chem. Sci 2018, 9, 7078–7090. [PubMed: 30310628]

(42). Stein BW; Morgenstern A; Batista ER; Birnbaum ER; Bone SE; Cary SK; Ferrier MG; John KD; Lezama Pacheco J; Kozimor SA; Mocko V; Scott BL; Yang P Advancing Chelation Chemistry for Actinium and Other +3 f-Elements, Am, Cm, and La. J. Am. Chem. Soc 2019, 141, 19404–19414. [PubMed: 31794205]

(43). Jones ZR; Livshits MY; White FD; Dalodière E; Ferrier MG; Lilley LM; Knope KE; Kozimor SA; Mocko V; Scott BL; Stein BW; Wacker JN; Woen DH Advancing Understanding of Actinide(iii) (Ac, Am, Cm) Aqueous Complexation Chemistry. Chem. Sci 2021, 12, 5638–5654. [PubMed: 34168798]

(44). Robertson AKH; McNeil BL; Yang H; Gendron D; Perron R; Radchenko V; Zeisler S; Causey P; Schaffer P ^{232}Th-Spallation-Produced ^{225}Ac with Reduced ^{227}Ac Content. Inorg. Chem 2020, 59, 12156–12165. [PubMed: 32677829]

(45). Ma D; McDevitt MR; Finn RD; Scheinberg DA Breakthrough of ^{225}Ac and Its Radionuclide Daughters from an ^{225}Ac/^{213}Bi Generator: Development of New Methods, Quantitative Characterization, and Implications for Clinical Use. Appl. Radiat. Isot 2001, 55, 667–678. [PubMed: 11573800]

(46). McDevitt MR; Finn RD; Sgouros G; Ma D; Scheinberg DA An ^{225}Ac/^{213}Bi Generator System for Therapeutic Clinical Applications: Construction and Operation. Appl. Radiat. Isot 1999, 50, 895–904. [PubMed: 10214708]

(47). Thiele NA; Woods JJ; Wilson JJ Implementing f-Block Metal Ions in Medicine: Tuning the Size Selectivity of Expanded Macrocycles. Inorg. Chem 2019, 58, 10483–10500. [PubMed: 31246017]

(48). Aluicio-Sarduy E; Thiele NA; Martin KE; Vaughn BA; Devaraj J; Olson AP; Barnhart TE; Wilson JJ; Boros E; Engle JW Establishing Radiolanthanum Chemistry for Targeted Nuclear Medicine Applications. Chem. - Eur. J 2020, 26, 1238–1242. [PubMed: 31743504]

(49). Hu A; Keresztes I; MacMillan SN; Yang Y; Ding E; Zipfel WR; DiStasio RA Jr.; Babich JW; Wilson JJ Oxyaapa: A Picolinate-Based Ligand with Five Oxygen Donors that Strongly Chelates Lanthanides. Inorg. Chem 2020, 59, 5116–5132. [PubMed: 32216281]

(50). Martell AE; Smith RM Critical Stability Constants; Plenum Press: New York, 1974; Vol. 1.

(51). Ramaiah NA; Tewari GD; Trivedi SR; Katiyar SS Spectrophotometric Titration of Bismuth with EDTA. Talanta 1968, 15, 352–356. [PubMed: 18960305]

(52). Lima LMP; Beyler M; Oukhatar F; Le Saec P; Faivre-Chauvet A; Platas-Iglesias C; Delgado R; Tripier R H_2Me-do2pa: An Attractive Chelator with Fast, Stable and Inert $^{nat}Bi^{3+}$ and $^{213}Bi^{3+}$ Complexation for Potential α-Radioimmunotherapy Applications. Chem. Commun 2014, 50, 12371–12374.

(53). Lima LMP; Beyler M; Delgado R; Platas-Iglesias C; Tripier R Investigating the Complexation of the Pb^{2+}/Bi^{3+} Pair with Dipicolinate Cyclen Ligands. Inorg. Chem 2015, 54, 7045–7057. [PubMed: 26146022]

(54). Wilson JJ; Ferrier M; Radchenko V; Maassen JR; Engle JW; Batista ER; Martin RL; Nortier FM; Fassbender ME; John KD; Birnbaum ER Evaluation of Nitrogen-Rich Macrocyclic Ligands for the Chelation of Therapeutic Bismuth Radioisotopes. Nucl. Med. Biol 2015, 42, 428–438. [PubMed: 25684650]

(55). Egorova BV; Matazova EV; Mitrofanov AA; Aleshin GY; Trigub AL; Zubenko AD; Fedorova OA; Fedorov YV; Kalmykov SN Novel Pyridine-Containing Azacrownethers for the Chelation of Therapeutic Bismuth Radioisotopes: Complexation Study, Radiolabeling, Serum Stability and Biodistribution. Nucl. Med. Biol 2018, 60, 1–10. [PubMed: 29499420]

(56). Šimeček J; Hermann P; Seidl C; Bruchertseifer F; Morgenstern A; Wester H-J; Notni J Efficient Formation of Inert Bi-213 Chelates by Tetraphosphorus Acid Analogues of DOTA: Towards Improved Alpha-Therapeutics. EJNMMI Res. 2018, 8, 78. [PubMed: 30091088]

(57). Matazova EV; Egorova BV; Konopkina EA; Aleshin GY; Zubenko AD; Mitrofanov AA; Karpov KV; Fedorova OA; Fedorov YV; Kalmykov SN Benzoazacrown Compound: A Highly

Effective Chelator for Therapeutic Bismuth Radioisotopes. MedChemComm 2019, 10, 1641–1645. [PubMed: 31814957]

(58). Bruchertseifer F; Comba P; Martin B; Morgenstern A; Notni J; Starke M; Wadepohl H First-Generation Bispidine Chelators for $^{213}Bi^{III}$ Radiopharmaceutical Applications. ChemMedChem 2020, 15, 1591–1600. [PubMed: 32613737]

(59). Lange JL; Davey PRWJ; Ma MT; White JM; Morgenstern A; Bruchertseifer F; Blower PJ; Paterson BM An Octadentate Bis(semicarbazone) Macrocycle: A Potential Chelator for Lead and Bismuth Radiopharmaceuticals. Dalton Trans. 2020, 49, 14962–14974. [PubMed: 33079111]

(60). Horváth D; Travagin F; Guidolin N; Buonsanti F; Tircsó G; Tóth I; Bruchertseifer F; Morgenstern A; Notni J; Giovenzana GB; Baranyai Z Towards ^{213}Bi Alpha-Therapeutics and beyond: Unravelling the Foundations of Efficient Bi^{III} Complexation by DOTP. Inorg. Chem. Front 2021, 8, 3893–3904.

SYNOPSIS.

The α-emitting radionuclides $^{225}Ac^{3+}$ and $^{213}Bi^{3+}$ are promising candidates for targeted alpha therapy (TAT), a form of nuclear medicine that harnesses α radiation to kill cancer cells. Here, we investigate the chelation of these radiometals with the ligands macrodipa and py-macrodipa to assess their suitability for TAT. In particular, py-macrodipa is demonstrated to be a promising candidate for $^{213}Bi^{3+}$ chelation, surpassing the current state-of-the art chelators macropa and DOTA.

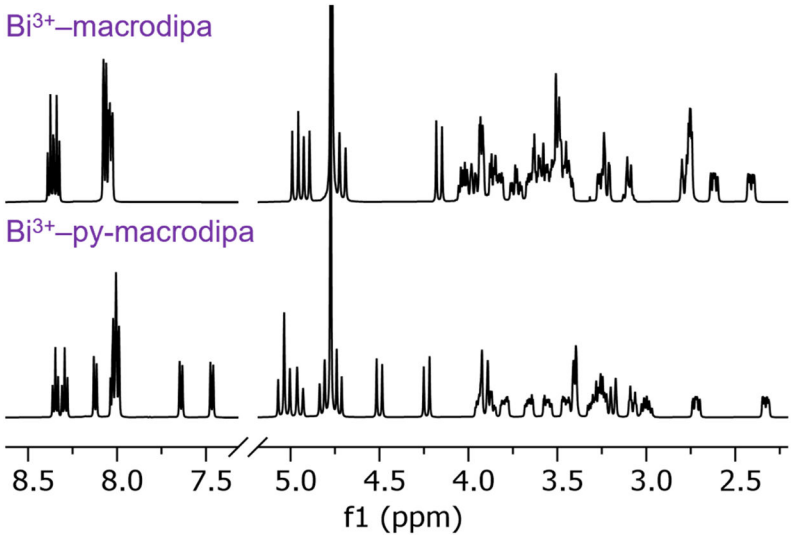

Figure 1.

^{1}H NMR spectra of Bi^{3+}–macrodipa and Bi^{3+}–py-macrodipa (500 MHz, D_2O, pD 5, 25 °C).

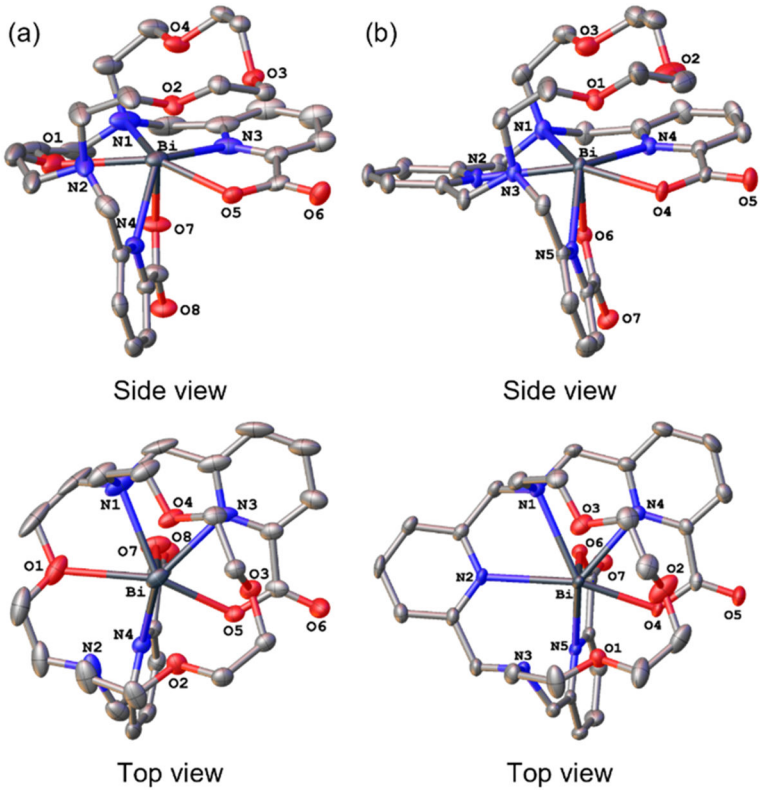

Figure 2.

Crystal structures of (a) $[Bi(macrodipa)]^+$ and (b) $[Bi(py\text{-}macrodipa)]^+$. Thermal ellipsoids are drawn at the 50% probability level. Solvent and counterions are omitted for clarity.

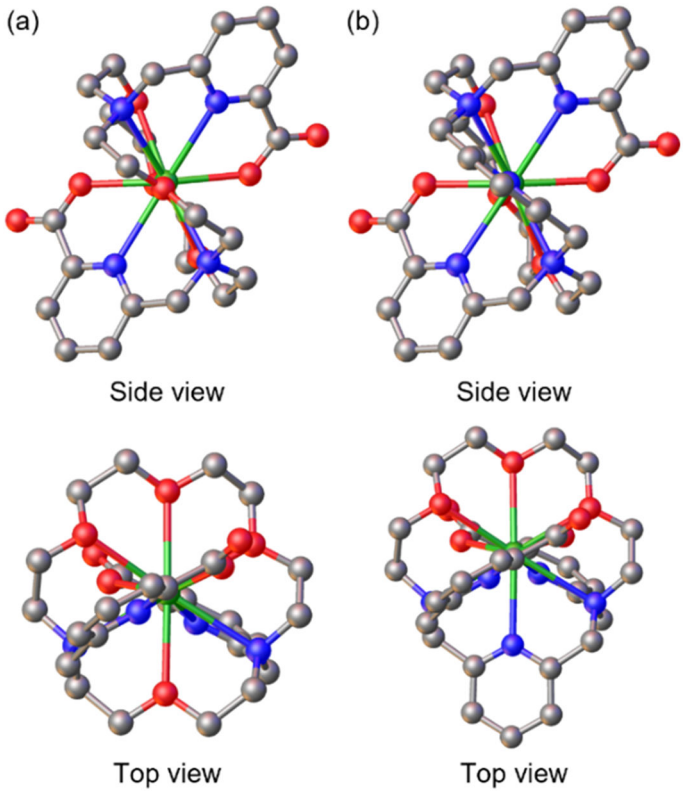

Figure 3.
DFT-optimized structures of (a) $[Ac(macrodipa)]^+$ and (b) $[Ac(py\text{-}macrodipa)]^+$. Hydrogen atoms are omitted for clarity. Green: Ac, grey: C, blue: N, red: O.

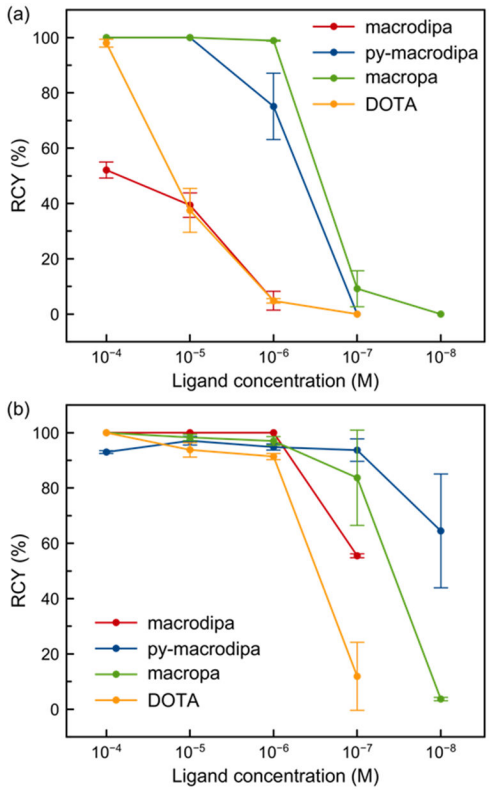

Figure 4.

Radiochemical yields at different ligand concentrations. (a) RCYs of $^{225}Ac^{3+}$ radiolabeling (25 °C for py-macrodipa, macropa, 40 °C for macrodipa, and 80 °C for DOTA; pH 5.5–6; 60 min reaction time). (b) RCYs of $^{213}Bi^{3+}$ labeling (25 °C for macrodipa, py-macrodipa, macropa and 95 °C for DOTA; pH 5.5–6; 6–8 min reaction time). Error bars represent the standard deviations. The $^{213}Bi^{3+}$ data with macropa and DOTA was taken from Ref 21.

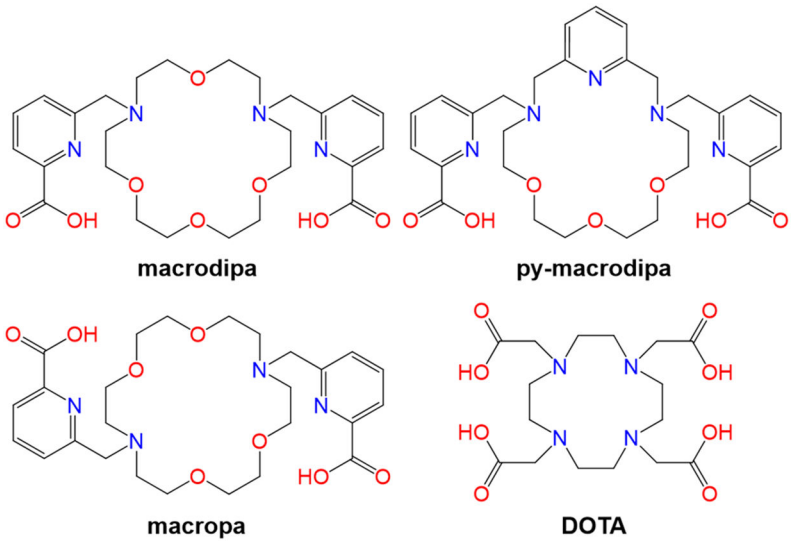

Chart 1.
Structures of Chelators Discussed in This Work.

Table 1.

Half-lives of Bi^{3+} Complexes when Challenged with 10 Equivalents of EDTA.[a]

	$t_{1/2}$
Bi^{3+}–macrodipa	9.2 ± 0.1 min
Bi^{3+}–py-macrodipa	13.2 ± 1.2 d
Bi^{3+}–macropa	2.2 ± 0.2 d

[a][BiL] = 100 μM, pH 5.0, 25 °C.